Anisotropic properties of the layered superconductor $Cu_{0.07}TiSe_2$

E. Morosan,[1] Lu Li,[2] N. P. Ong,[2] and R. J. Cava[1]
[1]*Department of Chemistry, Princeton University, Princeton, New Jersey 08540, USA*
[2]*Department of Physics, Princeton University, Princeton, New Jersey 08540, USA*
(Received 12 November 2006; published 12 March 2007)

The anisotropic superconducting properties of single crystals of $Cu_{0.07}TiSe_2$ were studied by measurements of magnetization and electrical resistivity. T_c is around 3.9 K, and the measured upper critical field (H_{c2}) values are ~1.25 and 0.8 T, for applied field parallel and perpendicular to the $TiSe_2$ planes, respectively. The anisotropy ratio $\gamma_{\text{anis}}=H_{c2}^{ab}/H_{c2}^{c}$ is close to 1.6 and nearly temperature independent. The lower critical field (H_{c1}) values are much smaller (~32 Oe for $H\|ab$ and 17 Oe for $H\|c$); demagnetizing corrections for field perpendicular to the thin plate crystals are required for the determination of H_{c1}^{c}. The anisotropy of the critical fields is described well by the anisotropic Ginzburg-Landau (GL) theory, and the characteristic GL parameters are determined and discussed.

DOI: 10.1103/PhysRevB.75.104505 PACS number(s): 74.25.Dw, 74.20.De, 74.25.−q

INTRODUCTION

$TiSe_2$ is one of the known charge-density wave (CDW) compounds,[1–5] with the CDW transition having been studied extensively due to its controversial nature. The crystal structure is that of the classical layered dichalcogenide type with hexagonal $TiSe_2$ layers stacked perpendicular to the crystallographic c axis. Cu intercalation between the $TiSe_2$ layers[6] has been recently shown to drive the CDW transition down in temperature and, at intermediate compositions ($x \geqslant 0.04$ in Cu_xTiSe_2), to give rise to a new superconducting (SC) state. After the CDW transition is fully suppressed for $x \geqslant 0.06$, the superconducting transition reaches a maximum value around $x=0.08$. This implies a competition between the two collective electron states (CDW and SC) that remains to be further elucidated.

Before the connection between the CDW and the SC states in Cu_xTiSe_2 can be understood, characterization of the SC state is of interest. Here, we report studies of platelike single crystals of $Cu_{0.07}TiSe_2$, allowing us to investigate the anisotropic physical properties of this system via magnetization and transport measurements. For $H\|ab$, the temperature dependence of the critical fields $H_{c1}(T)$ and $H_{c2}(T)$ are determined in a straightforward way. When field is applied perpendicular to the thin crystal plates (along the c axis), demagnetizing effects are considerable and must be taken into account. The upper critical field H_{c2}^{c} is almost unaffected by demagnetization, but the much smaller measured value of the lower critical field H_{c1}^{c} is significantly reduced from the effective field H_{c1}^{c*} in this orientation. After demagnetizing field corrections are applied, the anisotropic parameter characteristics of the superconducting state are determined and analyzed within the context of the anisotropic Ginzburg-Landau theory.

EXPERIMENT

Single crystals of $Cu_{0.07}TiSe_2$ were grown via chlorine vapor transport. Polycrystalline $TiSe_2$ powders were first synthesized by mixing stoichiometric amounts of Ti and Se powders and then heating them up to 650 °C at a rate of ~50 °/h in an evacuated silica tube. Next, $CuCl_2$ and $TiSe_2$ powders in a 0.10:1 ratio were sealed in 150-mm-long evacuated silica tubes with a 12 mm diameter. The tubes were placed in a gradient furnace with the hot temperature set at 650 °C and the cold end temperature kept at 550 °C. After 14 days, the furnace was cooled to room temperature over a few hours. Large hexagonal plates were formed toward the hot end.

X-ray diffraction measurements were employed to characterize the samples. Room-temperature data were recorded on a Bruker D8 diffractometer using a Cu $K\alpha$ radiation and a graphite diffracted beam monochromator. Magnetization measurements as a function of temperature and applied field $M(H,T)$ were performed in a Quantum Design Magnetic Properties Measurement System (MPMS) superconducting quantum interference device (SQUID) magnetometer ($T=1.8-350$ K, $H_{\max}=5.5$ T). Anisotropic resistivity $\rho(T,H)$ measurements with current parallel to the ab plane were taken in a ^{3}He refrigerator inserted in a 7 T superconducting magnet using a standard four-probe technique.

RESULTS

X-ray diffraction measurements on single crystals of $Cu_{0.07}TiSe_2$ showed them to have the structure previously reported on the polycrystalline materials. The copper content of 0.07 ± 0.01/f.u. was determined by the c lattice parameter calibration[6] and was consistent with the observed T_c of 3.9 K.

Figure 1 shows the $H=0$ resistivity data for $Cu_{0.07}TiSe_2$ as a function of temperature for the current flowing in the ab plane. At high temperatures, the resistivity is metallic in nature with $\rho(T)$ increasing almost linearly with T. Upon lowering the temperature, a superconducting transition occurs at $T_c=3.9$ K, as determined from the maximum slope of the resistivity around the transition (Fig. 1, upper inset). The 10–90% width of the resistive transition in zero field is 0.1 K. Just above the transition, the resistivity shows the quadratic behavior $\rho(T)=\rho_0+AT^2$ (Fig. 1, lower inset) expected for a Fermi liquid, with a residual resistivity $\rho_0=80$ $\mu\Omega$ cm and a coefficient $A\approx 1.1\times10^{-2}$ $\mu\Omega$ cm K^{-2}. ρ_0

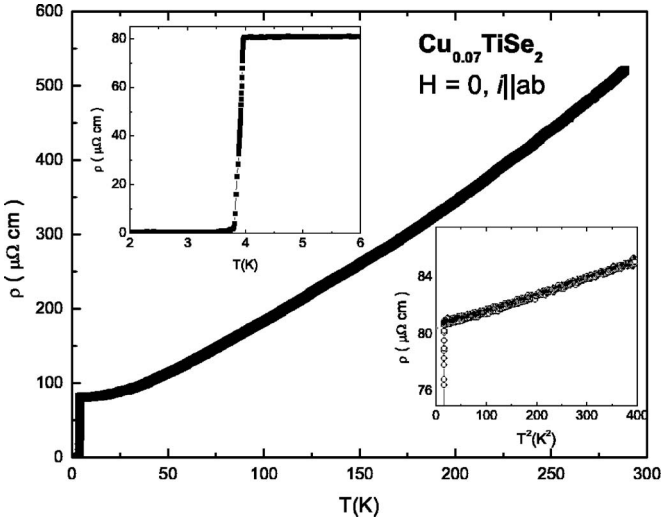

FIG. 1. $i\|ab$ temperature-dependent resistivity of $Cu_{0.07}TiSe_2$, with the low-temperature part shown in detail in the upper inset; lower inset: low temperatures $\rho(T^2)$ (symbols) with the linear fit (black line).

and $\rho(300\ \mathrm{K})$ are relatively large, about 80 and 520 $\mu\Omega$ cm, respectively, and the residual resistivity ratio (RRR) $=\rho(300\ \mathrm{K})/\rho(4.5\ \mathrm{K})$ is approximately 6.5. By comparison, superconducting layered $NbSe_2$ (Refs. 7 and 8) shows smaller $\rho(i\|ab)$ values (between 2 and 100 $\mu\Omega$ cm for 8 K $\leqslant T \leqslant 300$ K), resulting in a residual resistivity ratio (RRR) of approximately 40. We speculate that the intercalation of Cu atoms between the planes enhances the $i\|ab$ scattering processes compared to those observed in undoped layered structures (e.g., $NbSe_2$).

Anisotropic measurements of the field-dependent resistivity around the superconducting transition were performed down to ^{3}He temperatures. These results are shown in Fig. 2 for field applied parallel or perpendicular to the hexagonal plates. (The $TiSe_2$ planes are in the planes of the crystal plates.) In both cases, the current was parallel to the *ab* plane. For $H\|ab$ [Fig. 2(a)], the $T=0.35$ K $\rho(H)$ curve yields an upper critical field value $H_{c2}^{ab}=1.22$ T, as determined from the transition onset. An inflexion in the $\rho(H)$ data is observed around $H=1.3$ T, which moves lower in field as temperature increases. The origin of this feature is not known, but it may be associated with small inhomogeneities in the Cu doping concentration. The temperature dependence of H_{c2}^{ab} is characteristic of a type-II superconductor, as the transition moves to lower and lower field values upon increasing the temperature. Very similar behavior is observed for the other field orientation [$H\|c$, Fig. 2(b)] with smaller H_{c2}^{c} values. At $T=0.35$ K, $H_{c2}^{c}=0.71$ T, thus yielding an anisotropy ratio $\gamma_{\mathrm{anis}}=H_{c2}^{ab}/H_{c2}^{c}$ in $Cu_{0.07}TiSe_2$ of about 1.7.

Figure 3 shows the zero-field cooled $M(H)$ isotherms for field $H\|ab$ [Fig. 3(a)] and $H\|c$ [Fig. 3(b)]. These curves confirm the anisotropic suppression of the superconducting state observed in the magnetoresistance data. The minimum temperature available for these measurements is 1.8 K, where the $H\|ab$ magnetization becomes zero around $H_{c2}^{ab}(1.8\ \mathrm{K})\approx 0.96$ T. At the same temperature, the upper

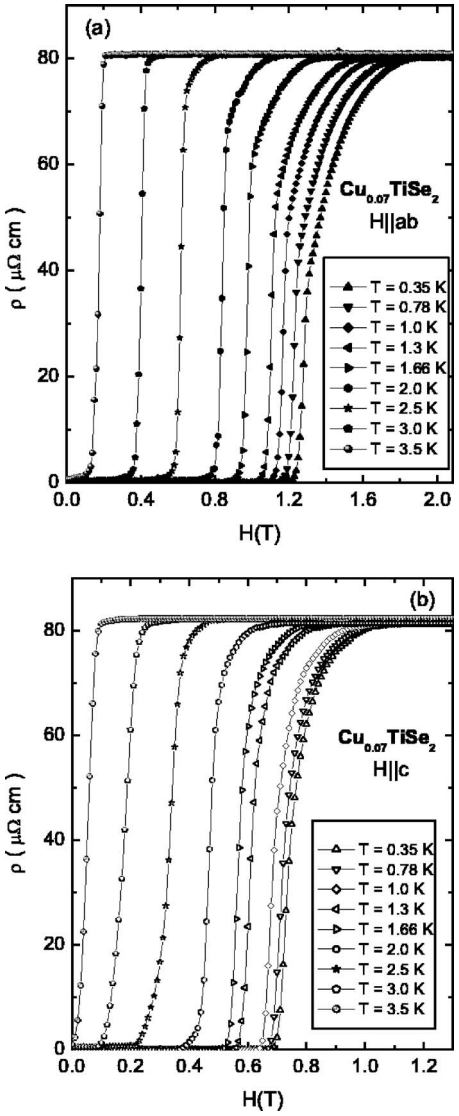

FIG. 2. Field-dependent magnetoresistance for (a) $H\|ab$ and (b) $H\|c$ at $T=0.35$, 0.78, 1.0, 1.3, 1.66, 2.0, 2.5, 3.0, and 3.5 K.

critical field H_{c2}^{c} in the *c* direction is determined to be 0.54 T. The insets in Fig. 3 show the magnetization in low magnetic fields from which the H_{c1} values can be estimated. For $H\|ab$ [inset, Fig. 3(a)], the $M(H)$ data are linear for very low fields (dotted line). H_{c1}^{ab} is determined as the point of departure from linearity, and these values are marked by vertical arrows for various temperatures. The analogous values are even smaller for $H\|c$ [inset, Fig. 3(b)], resulting in less accurate measurements of the magnetization values at such low fields. This allows us only to estimate the H_{c1}^{c} value at $T=1.8$ K (vertical arrow) as $\sim$13 Oe.

Based on our resistivity and magnetization measurements, the anisotropic properties of the superconducting state in $Cu_{0.07}TiSe_2$ can be summarized in a H_{c2}-T phase diagram [Fig. 4(a)]: the full symbols have been determined either from the $\rho(H)$ data (triangles) or $M(H)$ curves (circles) for $H\|ab$, and the open symbols correspond to the $H\|c$ direction. The inset shows the lower critical field values H_{c1} as determined from the $M(H)$ measurements. The dotted and

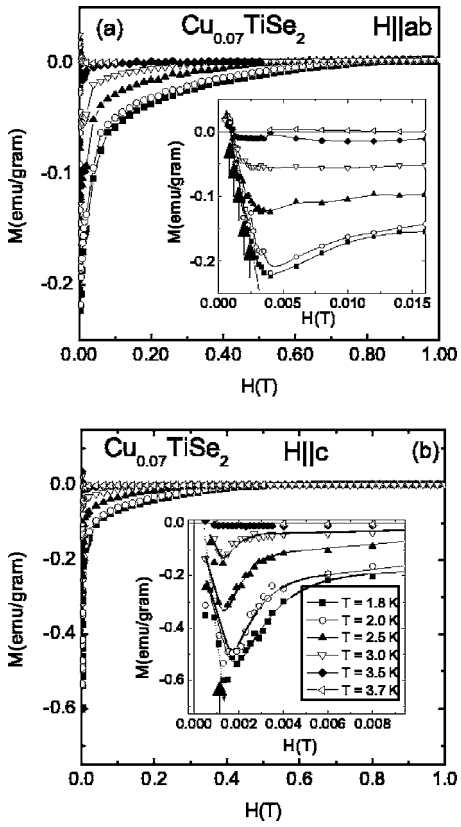

FIG. 3. Field-dependent magnetization isotherms for (a) $H\|ab$ and (b) $H\|c$ at $T=1.8$, 2.0, 2.5, 3.0, 3.5, and 3.7 K.

dashed lines represent fits in the $T\rightarrow 0$ and $T\rightarrow T_c$ regions, respectively. An almost temperature-independent anisotropy ratio $\gamma_{\text{anis}}=H_{c2}^{ab}/H_{c2}^{c}$ is observed [Fig. 4(b)].

DISCUSSION

As seen in Fig. 1, the $H=0$ resistivity data of $Cu_{0.07}TiSe_2$ show a superconducting transition around $T_c=3.9$ K. Above the transition, Fermi-liquid behavior is observed, characterized by quadratic dependence of the resistivity on temperature: $\rho(T)=\rho_0+AT^2$. The resistivity coefficient A is determined to be $\sim 1.1\times 10^{-2}\ \mu\Omega\ \text{cm/K}^2$. Using the $H=0$ electronic specific heat coefficient $\gamma=4.3\ \text{mJ/mol K}^2$,[6] the Kadowaki-Woods (KW) ratio A/γ^2 is estimated to be $\sim 60\times 10^{-5}\ \mu\Omega\ \text{cm/(mJ/mol K)}^2$. For many correlated electron systems, the Kadowaki-Woods ratio has been shown empirically to have a nearly universal value $a_0=10^{-5}\ \mu\Omega\ \text{cm/(mJ/mol K)}^2$ (solid line, Fig. 5).[9] A number of compounds have since been shown to follow on almost universal curves with either reduced (dotted line, Fig. 5) or enhanced (dashed lines, Fig. 5) KW ratios.[10,11] It can be seen that $Cu_{0.07}TiSe_2$ falls close to the $60a_0$ line, with many interme-

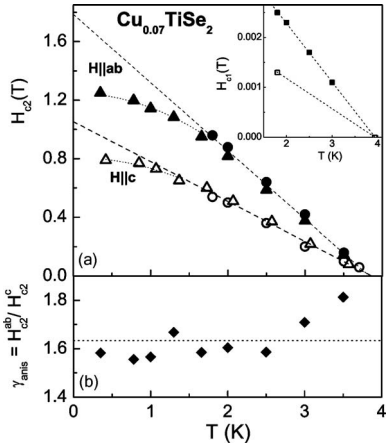

FIG. 4. (a) H_{c2}-T phase diagram of $Cu_{0.07}TiSe_2$, with $H_{c1}(T)$ shown in the inset. (b) The temperature dependence of the H_{c2} anisotropy ratio γ_{anis}.

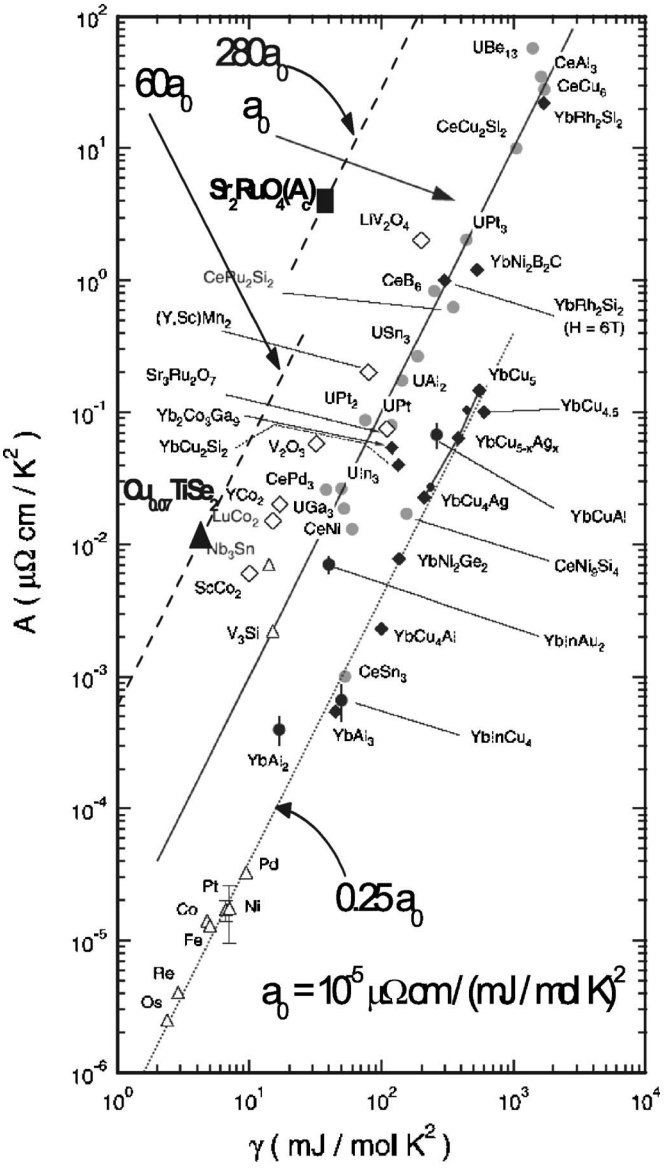

FIG. 5. A plot of the T^2 coefficient of the electrical resistivity A vs the electronic specific heat coefficient γ (reproduced from Ref. 10). The solid, dotted, and dashed lines represent $A/\gamma^2=a_0=1.0\times 10^{-5}\ \mu\Omega\ \text{cm mol}^2\ \text{K}^2/\text{mJ}^2$, $A/\gamma^2<a_0$, and $A/\gamma^2>a_0$, respectively. The large triangle (▲) corresponds to $Cu_{0.07}TiSe_2$ (present work) and the large square (■) corresponds to Sr_2RuO_4 (A_c) (Ref. 12).

TABLE I. Characteristic parameters of $Cu_{0.07}TiSe_2$: critical temperature for superconductivity T_c, residual resistivity ρ_0 near T_c, residual resistivity ratio (RRR), upper critical field $H_{c2}(0)$, GL coherence length $\xi(0)$, lower critical field $H_{c1}^*(0)$ (after the demagnetizing correction), anisotropy ratio of H_{c2} $\gamma_{anis}(0)$, GL parameter $\kappa(0)$, and GL penetration depth $\lambda(0)$. The $H\|c$ H_{c1} value (before applying the demagnetizing correction) was 13 Oe (see text).

	T_c (K)	ρ_0 ($\mu\Omega$ cm)	RRR	$H_{c2}(0)$ (T)	$\xi(0)$ (nm)	$H_{c1}^*(0)$[a] (Oe)	$\gamma_{anis}(0)$	$\kappa(0)$	$\lambda(0)$ (nm)
$H\|ab$				1.238	21.3	32		25	285
$H\|c$				0.729	12.5	53		13.4	584
	3.9	80	6.5				1.7		

[a] $H_{c1}^*=H_{c1}-N_dM$, where N_d represents the demagnetizing factor (see text).

tallic compounds falling in between the a_0 and the $60a_0$ lines. Various mechanisms have been proposed to explain the former universality class, such as intersite magnetic correlations or ground-state degeneracy. In Na_xCoO_2,[11] the KW ratio was found to be almost $50a_0$, which has been attributed to magnetic frustration, proximity to a magnetic quantum critical point, or a Mott transition. In the case of Sr_2RuO_4,[12] the KW ratio was found to be highly anisotropic, reaching values around $300a_0$ for current normal to the RuO_2 planes; this was attributed to the two-dimensional character of the Fermi liquid in this compound. Since the thin-plate geometry of the $Cu_{0.07}TiSe_2$ precluded us from performing transport measurements with current perpendicular to the $TiSe_2$ planes, we can only speculate that the Fermi liquid might have a two-dimensional character, possibly inducing the high KW ratio. Another possibility is the proximity of this compound to the transition from a CDW to a SC state, which may have significant influence on the scattering mechanism and, consequently, on the KW ratio.

Next, we analyze the superconducting state in $Cu_{0.07}TiSe_2$. The Bardeen-Cooper-Schrieffer (BCS) theory of superconductivity[13] predicts that for $T\rightarrow T_c$, the critical field behavior is almost linear in temperature. This is found for both field orientations for H_{c2} [Fig. 4(a)] in $Cu_{0.07}TiSe_2$ as well as for the $H\|ab$ H_{c1} values [inset, Fig. 4(a)] and emphasized by the dotted lines. As described previously, the small H_{c1}^c values correspond to very small measured magnetization values, making the accurate determination of the lower critical field difficult for this field orientation. In consequence, we are using the H_{c1}^c, determined at $T=1.8$ K, and $T_{c,H=0}=3.9$ K, as determined from the in-plane data to construct a dotted line analogous to that for $H\|ab$ [inset, Fig. 4(a)]. From the linear fits in the $H=0$ limit, the critical temperature is determined to be $T_c=3.9$ K; toward $T=0$, the extrapolations of these linear fits can be used to estimate the $H_{c2}(0)$ critical field values by using the Werthamer-Helfand-Hohenberg (WWH) equation,[14]

$$H_{c2}(0)=0.693[-(dH_{c2}/dT)]_{T_c}T_c.$$

Since the lower critical field values are only determined from magnetization measurements limited to temperatures above 1.8 K, we also use the WWH formula to estimate H_{c1} closer to $T=0$. The H_{c1} and H_{c2} values thus determined are listed in Table I: $H_{c1}^{ab}(0)\approx 32$ Oe, $H_{c1}^{ab}(0)\approx 17$ Oe, $H_{c2}^{ab}(0)\approx 1.23$ T, and $H_{c2}^{c}(0)\approx 0.73$ T. The anisotropy ratio of H_{c2}, calculated as $\gamma_{anis}(0)=H_{c2}^{ab}(0)/H_{c2}^{c}(0)$,[15] is also listed in Table I. In addition, the temperature dependence of γ_{anis} is shown in Fig. 4(b). For most of the superconducting state, γ_{anis} is almost constant and close to 1.63, except when very close to T_c where this value appears to be slightly higher; in this temperature range, H_{c1} and H_{c2} for both field orientations approach zero, and thus γ_{anis} is calculated as the ratio of two small quantities, and its determination is less certain. It can be concluded that the anisotropy γ_{anis} is intrinsically temperature independent.

Close to $T=0$, the upper critical field decreases with temperature as[13]

$$H_{c2}(T)\approx H_{c2}(0)[1-1.07(T/T_c)^2].$$

Fits to this expression are shown in Fig. 4(a) as dashed lines for both field orientations; for $H\|ab$, the resulting critical parameters are $H_{c2}^{ab}=1.24$ T and $T_c=3.6$ K, while for $H\|c$, $H_{c2}^{c}=0.8$ T and $T_c=3.4$ K. The estimated upper critical field values are close to those obtained before using the WWH formula, with the critical temperatures slightly smaller than the $T_c=3.9$ K, determined experimentally and from the linear fits.

The Ginzburg-Landau (GL) coherence length along the i direction ξ_i is estimated from the anisotropic GL formulas[16] for H_{c2}: $H_{c2}^{ab}=\Phi_0/(2\pi\xi_{ab}\xi_c)$ and $H_{c2}^{c}=\Phi_0/(2\pi\xi_{ab}^2)$, where Φ_0 is the flux quantum $\Phi_0=2.07\times10^{-7}$ G cm^{-2}. The anisotropic values of the coherence length $\xi_{ab}(0)$ and $\xi_c(0)$ are listed in Table I. The $T=0$ critical field values can also be used to determine the GL parameter $\kappa_i(0)$ along the i direction, using the equation $H_{c2}^i(0)/H_{c1}^i(0)=2\kappa_i^2(0)/\ln\kappa_i(0)$. In turn, the GL parameter $\kappa_i(0)$ is related to the coherence length $\xi_i(0)$ and the GL penetration depth $\lambda_i(0)$ as $\kappa_c(0)=\lambda_{ab}(0)/\xi_{ab}(0)$ and $\kappa_{ab}(0)=\lambda_{ab}(0)/\xi_c(0)=[\lambda_{ab}(0)\lambda_c(0)/\xi_{ab}(0)\xi_c(0)]^{1/2}$. These equations are used to determine the anisotropic $\lambda_i(0)$ values. Table I gives the GL estimates of $\kappa_i(0)$, $\xi_i(0)$, and $\lambda_i(0)$ for both field orientations ($H\|ab$ and $H\|c$). The anisotropic GL relations require that $\xi_{ab}/\xi_c=\lambda_c/\lambda_{ab}$. The coherence length values ξ_{ab} and ξ_c are 21.3 and 12.5 nm, respectively, resulting in a ratio of $\xi_{ab}/\xi_c\approx 1.7$, which is in excellent agreement to the H_{c2} anisotropy ratio $\gamma_{anis}(0)=H_{c2}^{ab}(0)/H_{c2}^{c}(0)\approx 1.7$. When comparing these ratios to that of the penetration depth values $\lambda_c/\lambda_{ab}=25.2/66$ nm≈ 0.4, it appears that the GL description of this system is invalid. However, the crystals of

$Cu_{0.07}TiSe_2$ are thin plates (thickness $d \approx 0.1$ mm, area $s \approx 10$ mm^2), and demagnetizing fields have a significant effect for field perpendicular to the plates. In what follows, we will take into account the demagnetizing effects in estimating the critical field values and determine the corresponding values for the affected GL characteristic parameters.

In general, the effective field H^{eff} is reduced from the applied magnetic field H^{app} by the demagnetizing field $H_d = N_d M$, where N_d represents the demagnetizing factor and M is the magnetization of the sample. For a thin plate, N_d is close to 0 when the applied field is parallel to the plate and almost 1 when the field is perpendicular to the plate. In the case of $Cu_{0.07}TiSe_2$, the demagnetizing correction to the applied magnetic field is negligible when $H \| ab$. Moreover, as H_{c2} is determined as the magnetic field where the sample enters the normal state, for which $M=0$, the measured H_{c2} values are very close to the effective upper critical field values. Thus, it appears that, of the critical fields for $Cu_{0.07}TiSe_2$, only the $H \| c$ H_{c1} value is significantly affected by demagnetizing effects. Figure 6 shows the $T=1.8$ K $H \| c$ magnetization data as a function of applied field (full symbols, top axis) and as a function of effective field $H^{\text{eff}} = H^{\text{app}} - M$ (open symbols, bottom axis). The effective value of the lower critical field H_{c1} is determined to be ~ 50 Oe. This yields a GL coefficient $\kappa_c(0)=13.4$, with corrected penetration depth values $\lambda_c = 584$ nm and $\lambda_{ab} = 285$ nm, and their ratio $\lambda_c/\lambda_{ab} = 584/285 \approx 2$. This is much closer to the ratio of the coherence lengths ξ_{ab}/ξ_c and the anisotropy ratio $\gamma_{\text{anis}}(0)=1.7$, as required by the GL theory.

In conclusion, we have shown that $Cu_{0.07}TiSe_2$ is a normal type-II superconductor, with a transition temperature $T_c = 3.9$ K. The superconducting state properties are anisotropic, characterized by an anisotropy ratio $\gamma_{\text{anis}}(0)=1.7$. In the normal state, the zero-field resistivity measurement yields a RRR around 7, but the overall resistivity values are high, indicative of high scattering mechanisms, possibly reflecting the intrinsically disordered nature of the intercalated copper atoms. Comparison to the layered $NbSe_2$ dichalcogenide superconductor,[17,18] which also shows moderate anisotropy $[H_{c2}^{ab}(0)/H_{c2}^{c}(0) \approx 3]$, is supportive of this idea, as the undoped layered $NbSe_2$ has lower in-plane resistivity values. A large A/γ^2 ratio is also observed for $Cu_{0.07}TiSe_2$, which may be due to the reduced dimensionality of the Fermi liquid or the proximity to the CDW-SC transition. Detailed studies of the Fermi surface in $Cu_{0.07}TiSe_2$ may provide further insight into the anisotropic properties observed in this intercalated layered superconductor.

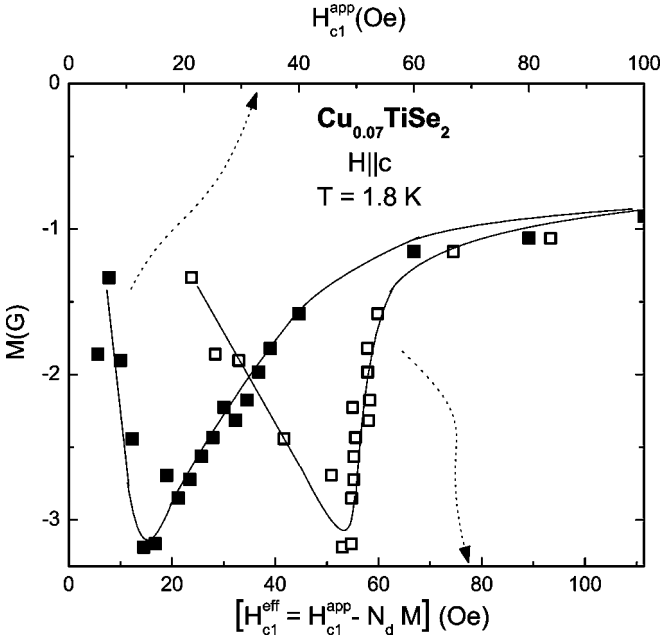

FIG. 6. Low field M_c data plotted as a function of applied field H_{c1}^{app} (full symbols) and effective field $H_{c1}^{\text{eff}} = H_{c1}^{\text{app}} - M$ (open symbols).

[1] K. C. Woo, F. C. Brown, W. L. McMillan, R. J. Miller, M. J. Schaffman, and M. P. Sears, Phys. Rev. B **14**, 3242 (1976).
[2] J. A. Wilson, Solid State Commun. **22**, 551 (1977).
[3] N. G. Stoffel, S. D. Kevan, and N. V. Smith, Phys. Rev. B **31**, 8049 (1985).
[4] A. Zunger and A. J. Freeman, Phys. Rev. B **17**, 1839 (1978).
[5] T. E. Kidd, T. Miller, M. Y. Chou, and T.-C. Chiang, Phys. Rev. Lett. **88**, 226402 (2002).
[6] E. Morosan, H. W. Zandbergen, B. S. Dennis, J. W. G. Bos, Y. Onose, T. Klimczuk, A. P. Ramirez, N. P. Ong, and R. J. Cava, Nat. Phys. **2**, 544 (2006).
[7] J. E. Edwards and R. F. Frindt, J. Phys. Chem. Solids **32**, 2217 (1971).
[8] H. N. S. Lee, H. McKinzie, D. S. Tannhauser, and A. Wold, J. Appl. Phys. **40**, 602 (1969).
[9] K. Kadowaki and S. B. Woods, Solid State Commun. **58**, 507 (1986).
[10] N. Tsujii, K. Yoshimura, and K. Kosuge, J. Phys.: Condens. Matter **15**, 1993 (2003).
[11] S. Y. Li, L. Taillefer, D. G. Hawthorn, M. A. Tanatar, J. Paglione, M. Sutherland, R. H. Hill, C. H. Wang, and X. H. Chen, Phys. Rev. Lett. **93**, 056401 (2004).
[12] Y. Maeno, K. Yoshida, H. Hashimoto, S. Nishizaki, S. Ikeda, M. Nohara, T. Fujita, A. P. Mackenzie, N. E. Hussey, J. G. Bednorz, and F. Lichtenberg, J. Phys. Soc. Jpn. **66**, 1405 (1997).
[13] J. Bardeen, L. N. Cooper, and J. R. Schrieffer, Phys. Rev. **108**, 1175 (1957).
[14] E. Helfand and N. R. Werthamer, Phys. Rev. **147**, 288 (1966); N. R. Werthamer, E. Helfand, and P. C. Hohenbegr, *ibid.* **147**, 295 (1966).
[15] M. Tinkham, *Introduction to Superconductivity* (McGraw-Hill, New York, 1996).
[16] J. R. Clem, Physica C **162-164**, 1137 (1989).
[17] P. de Trey, S. Gygax, and J.-P. Jan, J. Low Temp. Phys. **11**, 421 (1973).
[18] D. Sanchez, A. Junod, J. Muller, H. Berger, and F. Levy, Physica B **204**, 167 (1995).